

RESOURCE ARTICLE

Pulmonary transcriptome analysis in the surgically induced rabbit model of diaphragmatic hernia treated with fetal tracheal occlusion

Alexander C. Engels^{1,2}, Paul D. Brady³, Molka Kammoun³, Julio Finalet Ferreiro³, Philip DeKoninck^{1,2}, Masayuki Endo¹, Jaan Toelen^{1,4}, Joris R. Vermeesch³ and Jan Deprest^{1,2,*}

ABSTRACT

Congenital diaphragmatic hernia (CDH) is a malformation leading to pulmonary hypoplasia, which can be treated *in utero* by fetal tracheal occlusion (TO). However, the changes of gene expression induced by TO remain largely unknown but could be used to further improve the clinically used prenatal treatment of this devastating malformation. Therefore, we aimed to investigate the pulmonary transcriptome changes caused by surgical induction of diaphragmatic hernia (DH) and additional TO in the fetal rabbit model. Induction of DH was associated with 378 upregulated genes compared to controls when allowing a false-discovery rate (FDR) of 0.1 and a fold change (FC) of 2. Those genes were again downregulated by consecutive TO. But DH+TO was associated with an upregulation of 157 genes compared to DH and controls. When being compared to control lungs, 106 genes were downregulated in the DH group and were not changed by TO. Therefore, the overall pattern of gene expression in DH+TO is more similar to the control group than to the DH group. In this study, we further provide a database of gene expression changes induced by surgical creation of DH and consecutive TO in the rabbit model. Future treatment strategies could be developed using this dataset. We also discuss the most relevant genes that are involved in CDH.

KEY WORDS: RNA-seq, Congenital diaphragmatic hernia, CDH, Pulmonary hypoplasia, Tracheal occlusion, Fetoscopy

INTRODUCTION

The prevalence of congenital diaphragmatic hernia (CDH) ranges between 1-4/10,000 births, which translates to 542 to 2168 children in EU-27 member states every year (2008) (Kotecha et al., 2012). It can occur either as an isolated condition, associated with other anomalies or as part of a genetic syndrome. In CDH, lung development is disturbed already from the embryonic period, but progresses because of herniation of the viscera through the defect into the chest, competing for space with the developing lungs. As a consequence, lungs of babies with CDH have fewer and less mature airway branches, a smaller cross-sectional area of pulmonary vessels, remodeled vascular architecture, and an altered vasoreactivity

(Kinsella et al., 2005). At birth, this leads to respiratory insufficiency and persistent pulmonary hypertension (PPHT). This is lethal in up to 30% of cases, despite prenatal referral to high-volume centers that offer standardized neonatal care (Grushka et al., 2009; Hayakawa et al., 2013; van den Hout et al., 2011).

In countries with prenatal ultrasound (US) screening practices, >60% of cases are diagnosed at the latest by the second trimester. In isolated cases, an individualized prognosis can be made based on the degree of liver herniation and parenchymal lung size, predicting mortality and early neonatal morbidity (Cannie et al., 2008; Claus et al., 2011; Cruz-Martinez et al., 2011; Jani et al., 2007, 2009; Mayer et al., 2011; Ruano et al., 2012). The ability to prenatally identify a future non-survivor enables clinicians to propose a prenatal intervention that avoids this outcome. Today, the clinical method to stimulate lung development is fetal tracheal occlusion (TO). TO prevents egress of lung liquid, causing increased pulmonary stretch, which accelerates lung growth (DiFiore et al., 1994). This operation is currently evaluated within the framework of a randomized clinical trial, comparing fetoscopic endoluminal tracheal occlusion (FETO) to expectant management during pregnancy (Deprest et al., 2009, 2014).

Because TO still fails to save half of the fetuses with severe CDH and carries a risk for preterm delivery, there is a need for alternative prenatal strategies. Preclinical evaluation of these therapies involves the use of animal models, i.e. rodents, rabbits, and eventually lambs. Although, in all mammals, lung development progresses through five stages (embryonic, pseudoglandular, canalicular, sacular, alveolar), this is not at the same pace (Pringle, 1986). This needs to be kept in mind when choosing an animal model in studies on lung development. For instance, rodents are 'early' models because CDH is induced in the embryologic phase by the administration of a teratogen (Clugston et al., 2006; Keijzer et al., 2000). In these models, nitrofen (NF) is prenatally administered at embryonic day (E)11.5 (mice) or E13.5 (rats), and effects are studied at term, when lungs are in the canalicular to sacular phase (Beurskens et al., 2007; Correia-Pinto et al., 2010). All NF-exposed pups have lung hypoplasia, half of them also the diaphragmatic defect (Keijzer et al., 2000; Rottier and Tibboel, 2005; Schittny et al., 2000). These effects are believed to be caused by interference of NF with the retinoic acid (RA) signaling pathway, which is key in lung development (Malpel et al., 2000). This pathway is also disturbed in CDH in humans (Beurskens et al., 2009).

In larger animals, hypoplasia is induced by surgical creation of a diaphragmatic defect, typically in the pseudoglandular phase. Rabbits are widely available, have low housing needs, a timed gestation and large litter size. Rabbits alveolize *in utero* as in humans (Roubliova et al., 2010). Pups with diaphragmatic hernia (DH) display both histological and functional changes, such as reduced airway and vascular development, and pathologic compliance, airway resistance, tissue damping and elastance – mimicking the clinical phenotype (Flemmer et al., 2007; Roubliova et al., 2004; Wu

¹Department of Development and Regeneration, Organ System Cluster, Faculty of Medicine, KU Leuven, 3000 Leuven, Belgium. ²Clinical Department of Obstetrics and Gynaecology, Division Woman and Child, University Hospitals KU Leuven, 3000 Leuven, Belgium. ³Department of Human Genetics, Centre for Human Genetics, University Hospitals KU Leuven, 3000 Leuven, Belgium. ⁴Clinical Department of Pediatrics, Division Woman and Child, University Hospitals KU Leuven, 3000 Leuven, Belgium.

*Author for correspondence (jan.deprest@uzleuven.be)

This is an Open Access article distributed under the terms of the Creative Commons Attribution License (<http://creativecommons.org/licenses/by/3.0>), which permits unrestricted use, distribution and reproduction in any medium provided that the original work is properly attributed.

et al., 2000). Gene expression of a number of critical signaling molecules relevant to alveolarization, angiogenesis and regulation of vascular tone, but not to surfactant production, have been shown to be disrupted just as in humans (Vuckovic et al., 2013, 2012). However, a broader study on gene expression levels in this model has not been done so far. The use of RNA-sequencing (RNA-seq) for transcriptome analysis has become increasingly widespread with the advent of massively parallel sequencing technologies, in part owing to reductions in costs and increased throughput, and improved knowledge of non-model-organism reference genomes. Therefore, we wanted to investigate the pulmonary transcriptome after surgically induced DH creation and subsequent TO in the rabbit model. The provided gene expression database can be used to develop further treatment strategies for CDH.

RESULTS

At harvest, there were seven surviving DH+TO fetuses [mean lung-to-body weight ratio (LBWR): 0.017; standard deviation (s.d.): 0.002; confidence interval (CI) 95%: 0.013-0.022] and seven DH fetuses (mean LBWR: 0.011; s.d.: 0.003; CI 95%: 0.003-0.018). We also took one random control for every third litter (n=4) (mean LBWR: 0.016; s.d.: 0.001; CI 95%: 0.013-0.018). RNA integrity (RIN) values were determined, which led to the exclusion of one DH+TO fetus. All six remaining fetuses from the DH+TO group were analyzed. We selected four (DH) fetuses displaying the best RIN values (data not shown). Principal component analysis (PCA) and unsupervised hierarchical clustering revealed that three DH+TO samples clustered together as a single homogenous group, and two DH+TO samples clustered with the DH group. Those two samples correlate with a clinical sub-group of non-responders to the TO treatment, analysis of which was not the aim of our study. The remaining DH+TO sample was considered as a statistical outlier based upon quality control (QC) correlation analysis and calculation of modified allele dosage (MAD) scores using the Array Studio software (OmicSoft, Cary, USA); hence, it was excluded from further analysis. This distinct gene expression pattern of DH+TO fetuses correlated with two patterns of lung growth, as evidenced by the LBWR, which is a pathologic measure of the degree of lung development (Table 1).

Statistical inference analysis was performed between the groups defined above [DH (n=4), DH+TO (n=3) and control (n=4)] using

the general linear model function in Array Studio to calculate fold change (FC) values and false-discovery rate (FDR) values (applying the Benjamini–Hochberg procedure).

PCA and unsupervised hierarchical clustering of those dysregulated genes in any group comparison (described above) demonstrated clustering of homogenous groups for DH, DH+TO and control as expected, and revealed that DH+TO and control groups were more comparable than the DH group (Figs S1, S2).

The heat map generated by the unsupervised hierarchical clustering for the total of 641 unique genes found to be dysregulated (FC±2; FDR<0.1) in any group comparison is shown in Fig. 1. This reveals three large gene clusters whose expression values define the changes due to DH and after treatment with TO. The first gene cluster, containing 157 genes (Fig. 1, top) demonstrates low expression in both DH and control, and high expression in DH+TO only. This cluster represents genes whose expression is induced by TO, but which are unchanged in DH. The second, and largest, gene cluster, containing 378 genes (Fig. 1, mid) demonstrates high expression in DH only and low expression in control and DH+TO. This cluster represents genes whose expression is induced by DH, and which are reversed to lower levels by subsequent TO. The third gene cluster, containing 106 genes (Fig. 1, bot), demonstrates high expression in controls, and low expression in both DH and DH+TO. This cluster represents genes whose expression is reduced following DH, and which remain expressed at low levels even after TO.

To summarize, from the hierarchical cluster heat map shown in Fig. 1 it is apparent that the major change in gene expression (Fig. 1, gene cluster 2, mid) is upregulation of genes in DH, which are downregulated by TO towards, or beyond, levels seen in the controls (normal state) at the same developmental time point. One subset of genes is unchanged by TO and remains expressed at low levels, and one subset is highly upregulated by TO in comparison to both control and DH without TO.

The database of all dysregulated genes found in our study can be found in Table S1.

Pathway analysis

Analysis of the dysregulated gene sets for each comparison detailed above and for each of the gene clusters defined above was performed using the IPA web application (Ingenuity Pathway Analysis,

Table 1. Fetal body weight, total fetal lung weight, weight of the left lung, weight of the right lung and LBWR after harvesting at 30 days' gestational age of the three different groups (control, DH, DH+TO)

Group	Excluded	Total lung weight (g)	LL weight (g)	RL weight (g)	Body weight (g)	LBWR
DH	Yes	0.438	0.142	0.296	50.03	0.009
DH	Yes	0.558	0.172	0.386	46.62	0.012
DH	Yes	0.546	0.212	0.334	33.35	0.016
DH		0.506	0.121	0.385	36.14	0.014
DH		0.334	0.104	0.230	41.75	0.008
DH		0.399	0.128	0.271	36.27	0.011
DH		0.390	0.141	0.249	43.33	0.009
DH+TO	Yes	0.376	0.093	0.226	29.16	0.013
DH+TO	Yes	0.434	0.127	0.272	30.36	0.014
DH+TO	Yes	0.310	0.105	0.205	29.94	0.010
DH+TO	Yes	0.421	0.115	0.306	31.23	0.013
DH+TO		0.583	0.207	0.376	34.29	0.017
DH+TO		0.627	0.118	0.509	39.19	0.016
DH+TO		0.738	0.081	0.657	36.90	0.020
Control		0.546	0.235	0.311	36.41	0.015
Control		0.583	0.229	0.354	34.29	0.017
Control		0.512	0.257	0.276	34.13	0.015
Control		0.459	0.223	0.236	32.79	0.014

Excluded samples are specified. LL, left lung; RL, right lung; LBWR, lung-to-body weight ratio; DH, diaphragmatic hernia; TO, tracheal occlusion.

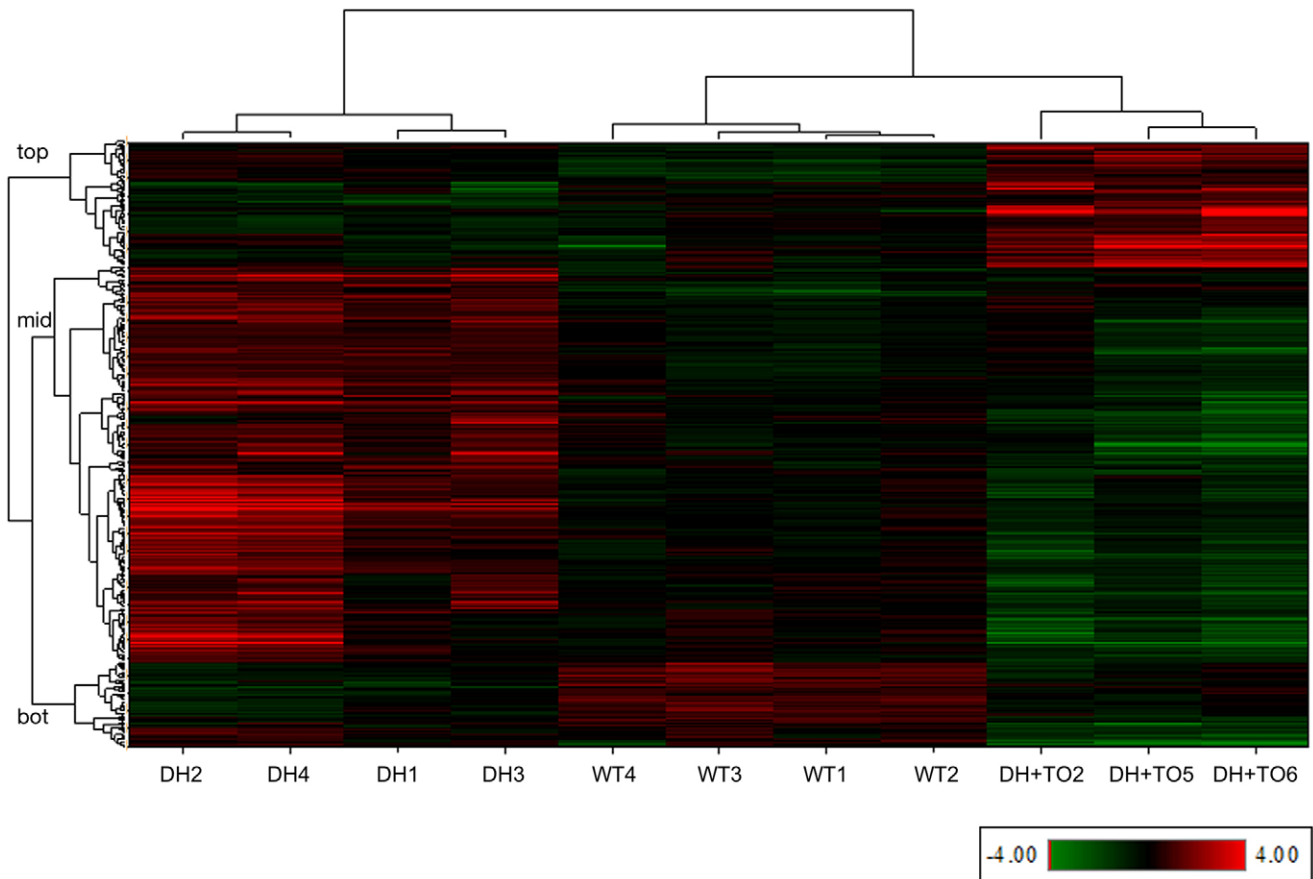


Fig. 1. Heat map generated by unsupervised hierarchical clustering of individual sample level data (Log₂-transformed RPKM expression values per gene) for the 641 unique genes found to be dysregulated in any group comparison, demonstrating that the different groups (DH, WT and TO) cluster together. Samples are clustered on the horizontal axis and genes on the vertical axis. Gene expression values are shown as red for high expression and green for low expression; intensity reflects the level. This reveals three large gene clusters, labeled as top, mid, bot. Information on gene names, fold changes (FC) and false-discovery rate (FDR) values for the group comparisons, and Gene Cluster and STEM profile number, are provided in Table S1. WT, control group.

Ingenuity Systems, Redwood City, CA, USA). Of the total 641 unique genes, 560 genes were mapped within IPA to known functional genes with human, mouse or rat homologs. This gene set was used to create a protein-protein interaction (PPI) network where experimental evidence supports direct interactions (i.e. predictions and indirect interactions were not allowed), and orphan molecules were subsequently removed. The resulting network is displayed in Fig. S3, where the molecules are colored according to the gene clusters identified in Fig. 1 (blue=genes with significantly increased expression in DH compared to DH+TO and/or control; yellow=genes with significantly increased expression in DH+TO compared to DH and/or control; and green=genes with significantly decreased expression in DH and/or DH+TO in comparison to control).

The Cytoscape plugin iRegulon (Janky et al., 2014) was used to identify potential transcription factors (TFs) of interest, using the 641 genes dysregulated in any comparison as the input. iRegulon searches for enrichment of cis-regulatory TF motifs in the target gene set, and predicted FOXJ1 as a key regulatory TF in our study. The input list contains 139/641 (22%) genes that are ‘target’ genes of FOXJ1.

In addition, we used the STEM application (Ernst and Bar-Joseph, 2006) to identify clusters of genes with similar changes in expression over time or, in our case, the changes observed from control to disease (DH) to treatment (DH+TO). The input was the FC values for the 641 genes significantly dysregulated in any

comparison, where time point 1 is control data (i.e. FC=1), time point 2 is the CDH vs control data, and time point 3 is the TO vs control data. This identified four significant clusters containing genes with similar changes in expression profile, of which Profile 9 contained the largest number of genes and was of highest significance (Fig. 2, and Table S2).

Real-time quantitative PCR (qPCR)

PCR analysis of ten of the 12 analyzed genes yielded results that were in agreement with RNA-seq data (Fig. S4). For eight genes, the differential expression between groups was concordant with the RNA-seq data ($P < 0.05$, Mann-Whitney U test). However, qPCR did not show a significant increase of *RFX3* and *LRRQ11* in the DH group compared to control (Fig. S5). For *BMPR2* and *PDE5A*, qPCR failed to show any difference between DH and wild type. This distinct gene expression pattern of DH+T fetuses correlated with two patterns of lung growth, as evidenced by the LBWR, which is a pathologic measure of the degree of lung development. However, *PDE5A* was significantly downregulated in the TO group.

DISCUSSION

In this study, we describe for the first time the pulmonary transcriptome analysis of specimens obtained in a rabbit model for pulmonary hypoplasia. The latter was induced by creating a diaphragmatic defect during the pseudoglandular phase. Conversely, forced lung growth was induced by fetal TO at the

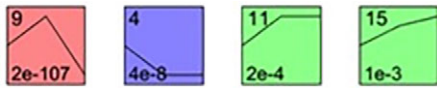


Fig. 2. The four significant gene profiles identified using the STEM application. Three 'time points' are visible on the plots, representing changes in expression of the respective gene clusters from controls (point 1) to DH (point 2), and DH treated with TO (point 3). Profile number (see Table 2) is displayed in the top left, *P*-value bottom left. The colors are to illustrate that the changes in expression are similar in profiles 11 and 15 but different from 9 and 4.

transition of the canalicular to saccular phase. We found that the largest group of genes that were significantly dysregulated were 378 genes that were both upregulated by DH creation and downregulated by TO to a level similar to that of controls. Furthermore, this study gives a database of genes that are significantly influenced by DH creation and consecutive TO (Table S1). This database can be used for further understanding of the disease process and development of treatment modalities for CDH. Below, we discuss some of the most relevant genes that we found were dysregulated.

Relation of findings to previous gene expression analytical experiments in other models of CDH and/or TO

Many studies have documented expression changes for numerous genes in association with CDH and, to a lesser extent, also the effects of TO, all of this in various animal models of CDH. This is typically done by using PCR for selected genes, or using broader arrays, at least for experiments done in (NF-exposed) rodents, a species in which molecular tools are abundantly available. Using a more modern technique such as RNA-seq, one can now also document and screen for changes in gene expression in relevant animal models for pulmonary hypoplasia and induced lung growth, even if the genome has not been completely identified. We herein used this technology in rabbits, and studied dysregulations associated with pulmonary hypoplasia and TO. The latter is done to force lung growth, which has been abundantly demonstrated in several animal models of CDH using other tools (Khan et al., 2007). In this experiment, we confirmed the effects of TO on cell proliferation. MKI67 is a key cell proliferation marker and was significantly upregulated by TO. The effect of TO was in proportion to the pre-existing lung size (FC 3.6056, FDR 0.0874; TO vs control), a phenomenon already clinically demonstrated (Peralta et al., 2008). Other genes related to the mechanisms of TO in previous studies were identified. To name only one, *AQP4* was upregulated in DH (FC 2.3562, FDR 0.018) yet went down to a normal level after TO (FC -2.7286 , FDR 0.0106). *AQP4* is a transport molecule that has previously been shown to be downregulated by stretch force on fetal lung AT2 cells *in vitro* (Wang et al., 2006).

TO is, however, in essence performed to enhance alveologenesis and reverse vascular changes that are typical of this disease. We observed dysregulation of connective tissue growth factor (*CTGF*). *CTGF* indeed enhances alveologenesis and microvascularization during late lung development (Hall-Glenn and Lyons, 2011). *CTGF* was earlier shown to be upregulated by TO in the saccular phase of E21 rats (Burgos et al., 2010; Mesas-Burgos et al., 2009). In line with that, *CTGF* was, in our rabbits, also firmly upregulated by TO (FC 2.8135, FDR 0.0151). The same dysregulation was observed for a number of other genes that have been previously associated with DH and TO. *BMPR2* expression was increased in DH (FC 1.9265, FDR 0.0228) and went down after TO (FC -2.7956 , FDR 0.0097). This gene encodes a member of the bone morphogenetic protein (BMP)

receptor family of transmembrane serine/threonine kinases and the ligands of this receptor are the BMPs, which are members of the TGF- β superfamily and are involved in embryogenesis. Disruption of *BMPR2* activity and downstream signaling has been demonstrated in the NF rodent model of CDH (Gosemann et al., 2013; Makanga et al., 2013). *BMPR2* plays a key role in pulmonary vasculogenesis during the late stages of fetal lung development and is essential for control of endothelial and smooth-muscle cell proliferation. Dysfunction of *BMPR2* and downstream signaling have been shown to disturb the crucial balance of proliferation of smooth muscle cells, contributing to the pathogenesis of human and experimental pulmonary hypoplasia (Gosemann et al., 2013; Makanga et al., 2013). In line with this was downregulation of *BMP7* in DH, yet significant upregulation by TO (FC 2.311, FDR 0.0163). *BMP7* was reportedly downregulated in the lungs of the NF rodent (Makanga et al., 2013).

We were, however, mainly interested in the RNA-seq technology because it has the potential to identify new targets that are involved in the condition and that can respond to prenatal intervention. One example is that DH in our rabbits was associated with a significant increase in *PDE5A* gene expression. The latter has been well documented in rodents and sheep, and it has been tied to the postnatal problem of pulmonary hypertension (Noori et al., 2007). The interesting observation here is that TO dramatically reduced *PDE5A* gene expression (FC -2.49 ; FDR 0.0097). *PDE5A* gene expression might also be altered by an alternative prenatal intervention, i.e. the transplacental administration of drugs. Sildenafil, which is already used to treat PPHT of the newborn (Noori et al., 2007), was recently shown to effectively inhibit cyclic guanosine monophosphate (cGMP)-specific phosphodiesterase type 5 *in utero* (Luong et al., 2011). In the latter experiment, NF rodents were used, and we confirmed a similar effect in rabbits, and others in the fetal lamb (Luong et al., 2011; Russo et al., 2015; Shue et al., 2014).

Future application: single cell-type populations

When starting from our RNA-seq data, the Cytoscape plugin iRegulon predicted that over 20% of dysregulated genes were target genes of *FOXJ1*. *FOXJ1* is a marker for ciliated cells; it is actually involved as a transcription factor in ciliogenesis (Yu et al., 2008). To our knowledge, it has so far not been named in DH. Our experiments demonstrate that DH rabbit pups display upregulation of *FOXJ1*, whereas it was downregulated after TO. Other ciliated-cell marker genes (*CCDC19*, *SPAG17*, *CCDC39*, *LRRIQ1*, *EFHC1*, *LRRC23*, *TTC18*, *WDR16*, *FANK1*, *ENKUR*, *CCDC113*) were also upregulated in DH lungs compared to controls, and downregulated by TO to levels lower than in controls. These findings point to an increased number of ciliated cells in DH lungs, which is reversed by TO. Loss of ciliated cells after TO has been previously described in the upper conducting airways in fetal lambs with CDH, although that study did not quantify changes in the more distant airways (Depest et al., 2000). The study of effects of DH and TO on the variety of individual lung cell types can benefit from modern technology such as single-cell RNA-seq (Treutlein et al., 2014). Those investigators applied this method to the developing distal lung epithelium in the mouse, which revealed a number of putative markers of ciliated cells, Clara cells, alveolar type 1 (AT1) cells and AT2 cells. A number of genes in our data are also present within the top 30 putative markers for each lung cell type (both known and novel) previously identified in the Treutlein et al. (2014) study (Table 2). For instance, the Clara cell markers *SCGB1A1*,

Table 2. Marker genes for different lung cell types that were revealed to be significantly dysregulated in one or more comparisons (DH vs control; DH+TO vs DH; DH+TO vs control)

Markers of lung cell types	DH vs control		DH+TO vs DH		DH+TO vs control		STEM profile
	FC	FDR	FC	FDR	FC	FDR	
AT2 cell markers							
<i>CD36</i>	-1.574	0.0645	-1.6024	0.0651	-2.5222	0.0445	-
<i>CHI3L1</i>	-2.6009	0.0656	1.3452	0.5505	-1.9335	0.3014	4
<i>DLK1</i>	3.1566	0.0754	1.6257	0.4332	5.1317	0.0969	15
AT1 cell markers							
<i>CLIC5</i>	1.4758	0.0638	-2.6291	0.0097	-1.7815	0.0827	9
<i>AHNAK</i>	1.5615	0.386	-4.6513	0.0266	-2.9787	0.1637	9
<i>LIMCH1</i>	1.3993	0.2078	-2.2892	0.0229	-1.636	0.2011	9
Clara cell markers							
<i>SCGB1A1</i>	1.2778	0.3533	-8.2686	0.0078	-6.4711	0.0151	-
<i>PPAP2B</i>	1.6128	0.0436	-2.1248	0.0142	-1.3174	0.3054	9
<i>KDR (VEGFR2)</i>	1.7819	0.0281	-2.321	0.0121	-1.3025	0.3262	9
Ciliated cell markers							
<i>FOXJ1</i>	1.5702	0.2284	-2.0111	0.0968	-1.2808	0.6416	9
<i>CCDC19</i>	1.4553	0.2369	-2.3	0.0366	-1.5805	0.2945	9
<i>SPAG17</i>	2.0341	0.024	-2.3987	0.0138	-1.1792	0.6012	9
<i>CCDC39</i>	2.0141	0.031	-3.1263	0.0107	-1.5522	0.2233	9
<i>LRRIQ1</i>	2.1908	0.0306	-3.2301	0.0123	-1.4744	0.311	9
<i>EFHC1</i>	1.5074	0.1071	-2.29	0.0181	-1.5191	0.2262	9
<i>LRRC23</i>	1.4244	0.3106	-2.4415	0.0412	-1.7141	0.2747	9
<i>TTC18</i>	1.7167	0.0702	-2.3818	0.0213	-1.3874	0.371	9
<i>WDR16</i>	1.3893	0.1488	-2.4702	0.0128	-1.7781	0.1077	9
<i>FANK1</i>	1.3534	0.3871	-2.2848	0.0523	-1.6882	0.2853	9
<i>ENKUR</i>	1.4917	0.2823	-2.5538	0.0422	-1.7119	0.2973	9
<i>CCDC113</i>	1.4899	0.1396	-2.4036	0.019	-1.6133	0.2064	9

Marker genes are defined from the top 30 known and novel putative marker genes reported by Treutlein et al. (2014). DH, diaphragmatic hernia; TO, tracheal occlusion; FC, fold change; FDR, false-discovery rate. The colors indicate change in expression, from green and gray (downregulation) through pink and red (upregulation).

PPAP2B and *KDR (VEGFR2)* were also upregulated in DH, and subsequently downregulated after TO. These findings are consistent with findings in rodents (Asabe et al., 1998; Santos et al., 2007).

Discordant findings and limitations

The above is a simplified interpretation and biased presentation of our results. First, we identified a number of discrepancies in results between rabbits and other models. For example, *AQP4*, *TGFBR3*, *EPAS1* and *TGFB-I* were upregulated in rabbits with CDH, whereas they were downregulated in the NF rat. In rodents, DH is induced early in gestation by a teratogen interfering directly with the RA pathway, whereas, in rabbits, a surgical defect is created beyond mid-gestation. This means that, in both models, different mechanisms or pathways are involved. Therefore, prenatal interventions might have different effects. For instance, maternal retinoic acid administration in rabbits does not affect the gross anatomical, morphological or proliferative characteristics (Gallot et al., 2008), whereas it rescues lungs in NF rats (Montedonico et al., 2006). Next to that there are also large differences between the time points in gestation and/or lung development at which prenatal interventions are done.

Actually, the largest effect measured was that for WNT inhibitor factor 1 (*WIF-1*) gene expression [up in DH (FC 8.8107, FDR 0.0153) and down after TO (FC -4.1432, FDR 0.0272)]. However, *WIF-1* downregulation was previously reported in the NF rodent lungs during the saccular stage of lung development (Fujiwara et al., 2012). WNT signaling plays an essential role in embryonic development. *WIF1* is a target gene of SMAD1 in the developing lung epithelial cells and acts to inhibit WNT proteins (Xu et al., 2011). SMAD1 plays a key role in organogenesis, including in lung development and maturation, and *SMAD1*-knockout mice display

reduced sacculation, which is an important feature of pulmonary hypoplasia (References?). How this needs to be tied together with our rabbit data remains unclear.

In addition, we observed changes that were different from what was previously described in clinical specimens. One example is that of the endothelin receptors EDNRA and EDNRB, which play a complex role in vascular tone. They are overexpressed in the thickened media of the pulmonary arteries of newborns with CDH (de Lagausie et al., 2005), as well as in the NF rodent model (Dingemann et al., 2010). Binding of endothelin 1 to its receptor EDNRA on pulmonary artery smooth-muscle cells results in vasoconstriction, whereas binding to the receptor EDNRB, present on endothelial cells, results in vasodilation mediated by endogenous nitric oxide. In our rabbit model, however, *EDNRB* was not differently expressed in DH as compared to controls.

We also observed discrepancies between the effects of DH and TO within the rabbit model. For instance c-fos induced growth factor [*FIGF*; also known as vascular endothelial growth factor D (*VEGFD*)] was downregulated in CDH as well as following TO. This is a member of the PDGF/VEGF family, and activates VEGFR2 and VEGFR3 receptors. Because it was not differentially expressed in the controls, we assume it was not involved. Conversely, VEGFR2 was upregulated in DH (FC 1.7819, FDR 0.0281) and down to normal levels after TO (FC -2.321, FDR 0.0121), which demonstrates the complex interactions of these factors.

We further had a number of discrepancies between RNA-seq and qPCR, which we touched upon already when reporting on results for *RF3X*, *LRRLQ1*, *BMP2* and *PDE5A*. Such discrepancies have been observed in previous reports (Duessa et al., 2013; Shi and He, 2014). This lack of concordance might be due to the poor knowledge of the rabbit genome and the absence of any single

nucleotide polymorphism (SNP) database, which could result in poor primer design for certain genes.

Additionally, we acknowledge several other limitations to our study. The sample size is small yet it matches financial limitations and is in line with the sample size of other studies analyzing the gene expression changes by TO in DH. Another is that the study of gene expression in whole lung samples will not detect changes occurring in individual cell types or different areas along the airways. These add to the generic limitations of translational studies in animal disease models, of which the clinical relevance remains uncertain. Another limitation of the study is that the surgical model does not fully recapitulate the etiology of the disease.

In conclusion, we first describe the pattern of dysregulated pulmonary gene expression in lungs of fetal rabbits with surgically induced DH. Interestingly, TO (tracheal occlusion), which is currently investigated as a prenatal surgical method to reverse pulmonary hypoplasia, is associated with a gene expression pattern that is comparable to what was observed in littermates with normal lung development.

MATERIALS AND METHODS

Surgery

The animal experiments were approved by the Ethics Committee of the Faculty of Medicine of the KU Leuven and all animals were treated according to current guidelines on animal wellbeing. In total, 12 does of New Zealand white rabbits (*Oryctolagus cuniculus*) were operated on and premedicated, after weight estimation, with ketamine 50 mg/kg body weight (Ketamine 1000 CEVA[®]; CEVA Santé Animale, Brussels, Belgium), xylazine 6 mg/kg body weight (Vexylan[®]; CEVA Santé Animale) and buprenorphine 0.03 mg/kg body weight (Vetergesic[®]; Reckitt Benckiser Healthcare, Brussels, Belgium), all injected intramuscularly. General anesthesia was maintained using isoflurane 1.5% (Isoba[®] Vet; Abbott Laboratories Ltd, Queensborough, Kent, UK) in oxygen at 1 liter/min via a facemask. Maternal heart rate and oxygen saturation were monitored with a pulse oxymeter (Nellcor[®] N-20P; Nellcor Inc., Haasrode, Belgium). Physiologic body temperature was maintained by a heating pad. The doe was placed in the supine position, the abdominal wall was shaved and disinfected with povidone iodine (Isobetadine[®]; Asta Medica, Brussels, Belgium) and covered with sterile drapes. Aseptic conditions were maintained throughout all surgical procedures. We operated on two fetuses in each doe, located in the middle of the left or right uterine horn. First diaphragmatic hernia (DH) was created at 23 days gestational age (GA). A second operation was performed at 28 days GA on the previously operated fetuses: either tracheal occlusion (DH+TO group), or sham neck dissection and skin closure (DH group). The latter is performed to include the effects of the fetal surgery *per se*. Before and after surgery, animals were housed in separate cages at normal room temperature and daylight, with free access to food and water. At 30 days GA, the does were euthanized with an intravenous bolus of a mixture of embutamide 200 mg, mebezonium 50 mg and tetracaine hydrochloride 5 mg (0.3 ml/kg T61; Marion Roussel Hoechst, Brussels, Belgium) after previous premedication as described above. All operated fetuses as well as one control unoperated littermate (control group) were euthanized *in utero* and harvested by cesarean section to obtain non-ventilated lungs.

Harvesting and sample preparation

During necropsy, the fetus and its lungs were weighed on a scale measuring accurately up to 0.001 g (HF 2000; A&D Instruments, Haasrode, Belgium) and the lung-to-body weight ratio (LBWR) was calculated.

Lung development is reflected by the LBWR and pathologists have defined critical cut-offs for pulmonary hypoplasia. We minimized contamination of the pulmonary tissue with other sources of DNA/RNA by flushing the lungs with saline by vascular access through the right ventricle of the fetal heart. The parenchymal lung tissue, i.e. without the trachea, was stored in RNAlater (Qiagen Benelux B.V., Venlo NL) at -4°C immediately.

RNA isolation

RNA isolation was performed on the entire left lung within 4 h of harvesting using the RNeasy mini kit (Qiagen Benelux B.V., Venlo NL). Tissue lysis and homogenization was performed in 1200 μl Buffer RLT using the TissueLyser system (Qiagen Benelux B.V., Venlo, The Netherlands). Following tissue disruption and homogenization, samples were centrifuged for 3 min at 8764 g (14,000 rpm) in a benchtop microcentrifuge. Lysate was transferred to fresh tubes and an equal volume of 70% ethanol was added. 600 μl of sample was added twice to a spin column, with two RNeasy spin columns used per sample. Following wash steps, RNA was eluted in 50 μl RNase-free H_2O .

Total RNA quantification was performed using the Nanodrop 1000 spectrophotometer (Thermo Scientific, Aalst, Belgium). RNA integrity was assessed using the RNA 6000 Nano Kit and the Bioanalyser (Agilent Technologies, Diegem, Belgium) according to the manufacturer's recommendations.

RNA-seq library preparation

One μg of total RNA was used as input material for sequencing library preparation, which was performed with the TruSeq RNA Library Preparation Kit (Illumina, Eindhoven, NL) according to the manufacturer's protocol. Fragmentation was performed for 6 min. Eight PCR cycles were used for the PCR enrichment step. Samples were indexed to allow for multiplexing. Sequencing libraries were quantified using the Qubit fluorometer (Life Technologies Europe B.V., Ghent, Belgium). Library quality and size range was assessed using the Bioanalyser (Agilent Technologies) with the DNA 1000 Kit (Agilent Technologies) according to the manufacturer's recommendations.

RNA-seq

Individual libraries were diluted to a final concentration of 2 nM and pooled for sequencing. Pooled libraries were sequenced in a single lane of an Illumina HiSeq2000 flow cell generating single end 50 bp reads. At least 10 million reads were obtained for all samples (range 12- to 32-million reads).

Data analysis

Fastq files were mapped to the rabbit genome and transcriptome (OryCun2.0 retrieved from Ensembl, release 69) with the Array Studio software (OmicSoft, Cary, NC, USA) using default parameters for single short read data. Between 72% and 78% of reads mapped uniquely to the reference genome and/or transcriptome, and a further 6% to 8% of reads mapped non-uniquely. Between 16% and 18% of reads were unmapped. Expression values were calculated per gene, normalized to 'reads per kilobase per million reads' (RPKM) values as previously described (Mortazavi et al., 2008). Data were filtered to remove those genes with expression of <1 RPKM in all samples. The RPKM expression values for the remaining 11,267 genes were subsequently Log₂ transformed for downstream PCA, hierarchical clustering, and for the subsequent calculation of fold changes (FC) by statistical inference analysis. All data are made available via ArrayExpress (accession number: E-MTAB-3452).

Hierarchical clustering

Hierarchical clustering was performed using the Array Studio software application, selecting 'Complete' for link option, and 'Correlation' for distance option. The 'Correlation' setting is also named 'Centered Pearson' $1-\text{corr}(x, y)$, and the source algorithms are further described in <http://cran.r-project.org/web/packages/amap/amap.pdf>. Clustering is based upon the Log-transformed RPKM gene expression values.

Downstream analysis

Downstream pathway analysis and creation of networks was performed using the IPA software application (Ingenuity Systems, Redwood City, CA, USA). The iRegulon plugin was used with the Cytoscape analysis software (<http://www.cytoscape.org/>) for prediction of upstream transcription factors of interest (Janky et al., 2014). The short time-series expression miner (STEM) application (Ernst and Bar-Joseph, 2006) was used to identify gene clusters with similar changes in expression between control and CDH, and following TO.

Real-time quantitative PCR (qPCR)

In order to confirm RNA-seq findings, we selected for qPCR (quantitative polymerase chain reaction) 12 genes with FC>2 or FC<(-2) and the housekeeping genes *SDHA*, *TOP1* and *GAPDH*, which were previously shown to be among the most stable genes in the CDH rabbit model and after TO (Vuckovic et al., 2013). PCR primers were designed using Primer 3 software and Primer-BLAST. The absence of secondary structure was checked by the Vector NTI program. All the primers were synthesized by Integrated DNA Technologies.

For a given gene, all samples were analyzed in the same qPCR run. 10- μ l reactions were prepared using 2 \times LightCycler 480 SYBR Green I Master (Roche Applied Science) with 2 μ l of a 1:10 cDNA dilution and a final concentration of 300 nM of each primer. Data were analyzed using the LightCycler 480 software (Roche Applied Science). The results were quantified using the comparative threshold cycle method as described by Livak and Schmittgen (2001). In addition, serial dilutions were used to create standard curves for relative quantification and the expression of each gene was normalized to at least two of the three housekeeping genes' expression. The sequences and the different primers and the corresponding PCR efficiencies are provided in Table S3.

Acknowledgements

We thank Rosita Kinnart and Ivan Laermans for their kind assistance in performing the animal experiments.

Competing interests

The authors declare no competing or financial interests.

Author contributions

A.C.E., P.D.B., J.T., J.R.V. and J.D.: study design and manuscript writing. A.C.E., P.D., M.E. and J.T.: performed the animal experiments. P.D.B., A.C.E., M.K., J.F.F., J.R.V. and J.D.: sequencing and analysis.

Funding

J.D. receives a fundamental clinical research grant of the Fonds Wetenschappelijk Onderzoek Vlaanderen (FWO; 18.01207). A.C.E. is supported by the Erasmus+ Program of the European Union (Framework agreement number 2013-0040; contract 1011990). This publication reflects the views only of the authors, and the European Commission cannot be held responsible for any use that may be made of the information contained therein.

Supplementary information

Supplementary information available online at <http://dmm.biologists.org/lookup/suppl/doi:10.1242/dmm.021626/-/DC1>

References

- Asabe, K., Tsuji, K., Handa, N., Kajiwara, M. and Suita, S. (1998). Expression of clara cell 10-kDa protein (CC10) in congenital diaphragmatic hernia. *Pediatr. Surg. Int.* **14**, 36-39.
- Beurskens, N., Klaassens, M., Rottier, R., de Klein, A. and Tibboel, D. (2007). Linking animal models to human congenital diaphragmatic hernia. *Birth Defects Res. A Clin. Mol. Teratol.* **79**, 565-572.
- Beurskens, L. W. J. E., Tibboel, D. and Steegers-Theunissen, R. P. M. (2009). Role of nutrition, lifestyle factors, and genes in the pathogenesis of congenital diaphragmatic hernia: human and animal studies. *Nutr. Rev.* **67**, 719-730.
- Burgos, C. M., Nord, M., Roos, A., Didon, L., Eklof, A.-C. and Frenckner, B. (2010). Connective tissue growth factor expression pattern in lung development. *Exp. Lung Res.* **36**, 441-450.
- Cannie, M., Jani, J., Chaffiotte, C., Vaast, P., Deruelle, P., Houfflin-Debarge, V., Dymarkowski, S. and Deprest, J. (2008). Quantification of intrathoracic liver herniation by magnetic resonance imaging and prediction of postnatal survival in fetuses with congenital diaphragmatic hernia. *Ultrasound Obstet. Gynecol.* **32**, 627-632.
- Claus, F., Sandaite, I., DeKoninck, P., Moreno, O., Cruz Martinez, R., Van Mieghem, T., Gucciardo, L., Richter, J., Michielsen, K., Decraene, J. et al. (2011). Prenatal anatomical imaging in fetuses with congenital diaphragmatic hernia. *Fetal Diagn. Ther.* **29**, 88-100.
- Clugston, R. D., Klattig, J., Englert, C., Clagett-Dame, M., Martinovic, J., Benachi, A. and Greer, J. J. (2006). Teratogen-induced, dietary and genetic models of congenital diaphragmatic hernia share a common mechanism of pathogenesis. *Am. J. Pathol.* **169**, 1541-1549.
- Correia-Pinto, J., Gonzaga, S., Huang, Y. and Rottier, R. (2010). Congenital lung lesions—underlying molecular mechanisms. *Semin. Pediatr. Surg.* **19**, 171-179.
- Cruz-Martinez, R., Hernandez-Andrade, E., Moreno-Alvarez, O., Done, E., Deprest, J. and Gratacos, E. (2011). Prognostic value of pulmonary Doppler to predict response to tracheal occlusion in fetuses with congenital diaphragmatic hernia. *Fetal Diagn. Ther.* **29**, 18-24.
- de Lagausie, P., de Buys-Roessingh, A., Ferkdadjji, L., Saada, J., Aisenfisiz, S., Martinez-Vinson, C., Fund, X., Cayuela, J. M., Peuchmaur, M., Mercier, J. C. et al. (2005). Endothelin receptor expression in human lungs of newborns with congenital diaphragmatic hernia. *J. Pathol.* **205**, 112-118.
- Deprest, J. A. M., Evrard, V. A., Verbeken, E. K., Perales, A. J., Delaere, P. R., Lerut, T. E. and Flageole, H. (2000). Tracheal side effects of endoscopic balloon tracheal occlusion in the fetal lamb model. *Eur. J. Obstet. Gynecol. Reprod. Biol.* **92**, 119-126.
- Deprest, J. A., Hyett, J. A., Flake, A. W., Nicolaidis, K. and Gratacos, E. (2009). Current controversies in prenatal diagnosis 4: should fetal surgery be done in all cases of severe diaphragmatic hernia? *Prenat. Diagn.* **29**, 15-19.
- Deprest, J., Brady, P., Nicolaidis, K., Benachi, A., Berg, C., Vermeesch, J., Gardener, G. and Gratacos, E. (2014). Prenatal management of the fetus with isolated congenital diaphragmatic hernia in the era of the TOTAL trial. *Semin. Fetal Neonatal Med.* **19**, 338-348.
- DiFiore, J. W., Fauza, D. O., Slavin, R., Peters, C. A., Fackler, J. C. and Wilson, J. M. (1994). Experimental fetal tracheal ligation reverses the structural and physiological effects of pulmonary hypoplasia in congenital diaphragmatic hernia. *J. Pediatr. Surg.* **29**, 248-256; discussion 256-257.
- Dingemans, J., Doi, T., Rutenstock, E. and Puri, P. (2010). Upregulation of endothelin receptors A and B in the nitrofen induced hypoplastic lung occurs early in gestation. *Pediatr. Surg. Int.* **26**, 65-69.
- Duressa, D., Anchieta, A., Chen, D., Klimes, A., Garcia-Pedrajas, M. D., Dobinson, K. F. and Klosterman, S. J. (2013). RNA-seq analyses of gene expression in the microsclerotia of *Verticillium dahliae*. *BMC Genomics* **14**, 607.
- Ernst, J. and Bar-Joseph, Z. (2006). STEM: a tool for the analysis of short time series gene expression data. *BMC Bioinformatics* **7**, 191.
- Flemmer, A. W., Jani, J. C., Bergmann, F., Muensterer, O. J., Gallot, D., Hajek, K., Sugawara, J., Till, H. and Deprest, J. A. (2007). Lung tissue mechanics predict lung hypoplasia in a rabbit model for congenital diaphragmatic hernia. *Pediatr. Pulmonol.* **42**, 505-512.
- Fujiwara, N., Doi, T., Gosemann, J.-H., Kutasy, B., Friedmacher, F. and Puri, P. (2012). Smad1 and WIF1 genes are downregulated during sacular stage of lung development in the nitrofen rat model. *Pediatr. Surg. Int.* **28**, 189-193.
- Gallot, D., Coste, K., Jani, J., Roubliova, X., Marceau, G., Velemir, L., Verheyen, A., Lemery, D., Sapin, V. and Deprest, J. A. (2008). Effects of maternal retinoic acid administration in a congenital diaphragmatic hernia rabbit model. *Pediatr. Pulmonol.* **43**, 594-603.
- Gosemann, J.-H., Friedmacher, F., Fujiwara, N., Alvarez, L. A. J., Corcionivoschi, N. and Puri, P. (2013). Disruption of the bone morphogenetic protein receptor 2 pathway in nitrofen-induced congenital diaphragmatic hernia. *Birth Defects Res. B Dev. Reprod. Toxicol.* **98**, 304-309.
- Grushka, J. R., Laberge, J.-M., Puligandla, P. and Skarsgard, E. D. (2009). Effect of hospital case volume on outcome in congenital diaphragmatic hernia: the experience of the Canadian Pediatric Surgery Network. *J. Pediatr. Surg.* **44**, 873-876.
- Hall-Glenn, F. and Lyons, K. M. (2011). Roles for CCN2 in normal physiological processes. *Cell. Mol. Life. Sci.* **68**, 3209-3217.
- Hayakawa, M., Ito, M., Hattori, T., Kanamori, Y., Okuyama, H., Inamura, N., Takahashi, S., Nagata, K., Taguchi, T., Usui, N. et al. (2013). Effect of hospital volume on the mortality of congenital diaphragmatic hernia in Japan. *Pediatr. Int.* **55**, 190-196.
- Jani, J., Nicolaidis, K. H., Keller, R. L., Benachi, A., Peralta, C. F. A., Favre, R., Moreno, O., Tibboel, D., Lipitz, S., Eggink, A. et al. (2007). Observed to expected lung area to head circumference ratio in the prediction of survival in fetuses with isolated diaphragmatic hernia. *Ultrasound Obstet. Gynecol.* **30**, 67-71.
- Jani, J. C., Benachi, A., Nicolaidis, K. H., Allegaert, K., Gratacos, E., Mazkereth, R., Matis, J., Tibboel, D., Van Heijst, A., Storme, L. et al. (2009). Prenatal prediction of neonatal morbidity in survivors with congenital diaphragmatic hernia: a multicenter study. *Ultrasound Obstet. Gynecol.* **33**, 64-69.
- Janky, R., Verfaillie, A., Imrichová, H., Van de Sande, B., Standaert, L., Christiaens, V., Hulselmans, G., Herten, K., Naval Sanchez, M., Potier, D. et al. (2014). iRegulon: from a gene list to a gene regulatory network using large motif and track collections. *PLoS Comput. Biol.* **10**, e1003731.
- Keijzer, R., Liu, J., Deimling, J., Tibboel, D. and Post, M. (2000). Dual-hit hypothesis explains pulmonary hypoplasia in the nitrofen model of congenital diaphragmatic hernia. *Am. J. Pathol.* **156**, 1299-1306.
- Khan, P. A., Cloutier, M. and Piedboeuf, B. (2007). Tracheal occlusion: a review of obstructing fetal lungs to make them grow and mature. *Am. J. Med. Genet. C Semin. Med. Genet.* **145C**, 125-138.
- Kinsella, J. P., Ivy, D. D. and Abman, S. H. (2005). Pulmonary vasodilator therapy in congenital diaphragmatic hernia: acute, late, and chronic pulmonary hypertension. *Semin. Perinatol.* **29**, 123-128.
- Kotecha, S., Barbato, A., Bush, A., Claus, F., Davenport, M., Delacourt, C., Deprest, J., Eber, E., Frenckner, B., Greenough, A. et al. (2012). Congenital diaphragmatic hernia. *Eur. Respir. J.* **39**, 820-829.

- Livak, K. J. and Schmittgen, T. D. (2001). Analysis of relative gene expression data using real-time quantitative PCR and the $2^{-\Delta\Delta C(T)}$ Method. *Methods* **25**, 402-408.
- Luong, C., Rey-Perra, J., Vadivel, A., Gilmour, G., Sauve, Y., Koonen, D., Walker, D., Todd, K. G., Gressens, P., Kassiri, Z. et al. (2011). Antenatal sildenafil treatment attenuates pulmonary hypertension in experimental congenital diaphragmatic hernia. *Circulation* **123**, 2120-2131.
- Makanga, M., Dewachter, C., Maruyama, H., Vuckovic, A., Rondelet, B., Naeije, R. and Dewachter, L. (2013). Downregulated bone morphogenetic protein signaling in nitrofen-induced congenital diaphragmatic hernia. *Pediatr. Surg. Int.* **29**, 823-834.
- Malpel, S., Mendelsohn, C. and Cardoso, W. V. (2000). Regulation of retinoic acid signaling during lung morphogenesis. *Development* **127**, 3057-3067.
- Mayer, S., Klaritsch, P., Petersen, S., Done, E., Sandaite, I., Till, H., Claus, F. and Deprest, J. A. (2011). The correlation between lung volume and liver herniation measurements by fetal MRI in isolated congenital diaphragmatic hernia: a systematic review and meta-analysis of observational studies. *Prenat. Diagn.* **31**, 1086-1096.
- Mesas-Burgos, C., Nord, M., Didon, L., Eklöf, A.-C. and Frenckner, B. (2009). Gene expression analysis after prenatal tracheal ligation in fetal rat as a model of stimulated lung growth. *J. Pediatr. Surg.* **44**, 720-728.
- Montedonico, S., Nakazawa, N. and Puri, P. (2006). Retinoic acid rescues lung hypoplasia in nitrofen-induced hypoplastic foetal rat lung explants. *Pediatr. Surg. Int.* **22**, 2-8.
- Mortazavi, A., Williams, B. A., McCue, K., Schaeffer, L. and Wold, B. (2008). Mapping and quantifying mammalian transcriptomes by RNA-Seq. *Nat. Methods* **5**, 621-628.
- Noori, S., Friedlich, P., Wong, P., Garingo, A. and Seri, I. (2007). Cardiovascular effects of sildenafil in neonates and infants with congenital diaphragmatic hernia and pulmonary hypertension. *Neonatology* **91**, 92-100.
- Peralta, C. F. A., Jani, J. C., Van Schoubroeck, D., Nicolaidis, K. H. and Deprest, J. A. (2008). Fetal lung volume after endoscopic tracheal occlusion in the prediction of postnatal outcome. *Am. J. Obstet. Gynecol.* **198**, 60.e1-60.e5.
- Pringle, K. C. (1986). Human fetal lung development and related animal models. *Clin. Obstet. Gynecol.* **29**, 502-513.
- Rottier, R. and Tibboel, D. (2005). Fetal lung and diaphragm development in congenital diaphragmatic hernia. *Semin. Perinatol.* **29**, 86-93.
- Roubliova, X., Verbeken, E., Wu, J., Yamamoto, H., Lerut, T., Tibboel, D. and Deprest, J. (2004). Pulmonary vascular morphology in a fetal rabbit model for congenital diaphragmatic hernia. *J. Pediatr. Surg.* **39**, 1066-1072.
- Roubliova, X. I., Deprest, J. A., Biard, J. M., Ophalvens, L., Gallot, D., Jani, J. C., Van de Ven, C. P., Tibboel, D. and Verbeken, E. K. (2010). Morphologic changes and methodological issues in the rabbit experimental model for diaphragmatic hernia. *Histol. Histopathol.* **25**, 1105-1116.
- Ruano, R., Takashi, E., da Silva, M. M., Campos, J. A. D. B., Tannuri, U. and Zugaib, M. (2012). Prediction and probability of neonatal outcome in isolated congenital diaphragmatic hernia using multiple ultrasound parameters. *Ultrasound Obstet. Gynecol.* **39**, 42-49.
- Russo, F., MiYague, A. H., Eastwood, P., DeKoninck, P., Van de Velde, G., Allegaert, K., Himmelreich, U., Toelen, J., Vergani, P. and Deprest, J. (2015). Transplacental sildenafil rescues vascular and airway morphometry in the rabbit model of congenital diaphragmatic hernia. In *35th Annual Meeting of the Society for Maternal-Fetal Medicine*, vol. 212, pp. S44-S45. San Diego.
- Santos, M., Nogueira-Silva, C., Baptista, M. J., Soares-Fernandes, J., Moura, R. S. and Correia-Pinto, J. (2007). Pulmonary epithelial cell differentiation in the nitrofen-induced congenital diaphragmatic hernia. *J. Pediatr. Surg.* **42**, 1231-1237.
- Schittny, J. C., Miserocchi, G. and Sparrow, M. P. (2000). Spontaneous peristaltic airway contractions propel lung liquid through the bronchial tree of intact and fetal lung explants. *Am. J. Respir. Cell Mol. Biol.* **23**, 11-18.
- Shi, Y. and He, M. (2014). Differential gene expression identified by RNA-Seq and qPCR in two sizes of pearl oyster (*Pinctada fucata*). *Gene* **538**, 313-322.
- Shue, E. H., Schecter, S. C., Gong, W., Etemadi, M., Johengen, M., Iqbal, C., Derderian, S. C., Oishi, P., Fineman, J. R. and Miniati, D. (2014). Antenatal maternally-administered phosphodiesterase type 5 inhibitors normalize eNOS expression in the fetal lamb model of congenital diaphragmatic hernia. *J. Pediatr. Surg.* **49**, 39-45; discussion 45.
- Treutlein, B., Brownfield, D. G., Wu, A. R., Neff, N. F., Mantalas, G. L., Espinoza, F. H., Desai, T. J., Krasnow, M. A. and Quake, S. R. (2014). Reconstructing lineage hierarchies of the distal lung epithelium using single-cell RNA-seq. *Nature* **509**, 371-375.
- van den Hout, L., Schaible, T., Cohen-Overbeek, T. E., Hop, W., Siemer, J., van de Ven, K., Wessel, L., Tibboel, D. and Reiss, I. (2011). Actual outcome in infants with congenital diaphragmatic hernia: the role of a standardized postnatal treatment protocol. *Fetal Diagn. Ther.* **29**, 55-63.
- Vuckovic, A., Roubliova, X. I., Votino, C., Naeije, R. and Jani, J. C. (2012). Signaling molecules in the fetal rabbit model for congenital diaphragmatic hernia. *Pediatr. Pulmonol.* **47**, 1088-1096.
- Vuckovic, A., Herber-Jonat, S., Flemmer, A. W., Roubliova, X. I. and Jani, J. C. (2013). Alveolarization genes modulated by fetal tracheal occlusion in the rabbit model for congenital diaphragmatic hernia: a randomized study. *PLoS ONE* **8**, e69210.
- Wang, Y., Maciejewski, B. S., Weissmann, G., Silbert, O., Han, H. and Sanchez-Esteban, J. (2006). DNA microarray reveals novel genes induced by mechanical forces in fetal lung type II epithelial cells. *Pediatr. Res.* **60**, 118-124.
- Wu, J., Yamamoto, H., Gratacos, E., Ge, X., Verbeken, E., Sueishi, K., Hashimoto, S., Vanamo, K., Lerut, T. and Deprest, J. (2000). Lung development following diaphragmatic hernia in the fetal rabbit. *Hum. Reprod.* **15**, 2483-2488.
- Xu, B., Chen, C., Chen, H., Zheng, S. G., Bringas, P., Jr, Xu, M., Zhou, X., Chen, D., Umans, L., Zwijsen, A. et al. (2011). Smad1 and its target gene Wif1 coordinate BMP and Wnt signaling activities to regulate fetal lung development. *Development* **138**, 925-935.
- Yu, X., Ng, C. P., Habacher, H. and Roy, S. (2008). Foxj1 transcription factors are master regulators of the motile ciliogenic program. *Nat. Genet.* **40**, 1445-1453.

Supplementary Table 1: Dataset of dysregulated genes identified from the study. The table provides details of all those genes which were identified as dysregulated in one or more group comparisons. Columns display the Ensembl Gene ID (Rabbit; *Oryctolagus cuniculus*); the Gene Symbol (where available). Fold Change and False Discovery Rates (FDR_BH) are given for each group comparison; CDH vs Control; TO vs CDH; TO vs Control. Genes are sorted by the 3 gene clusters (Heatmap Cluster) identified from the hierarchical clustering heatmap shown in Figure 1 and described in the main text. Those genes contained within the significant STEM profiles (see main text) are also labelled with the STEM profile number.

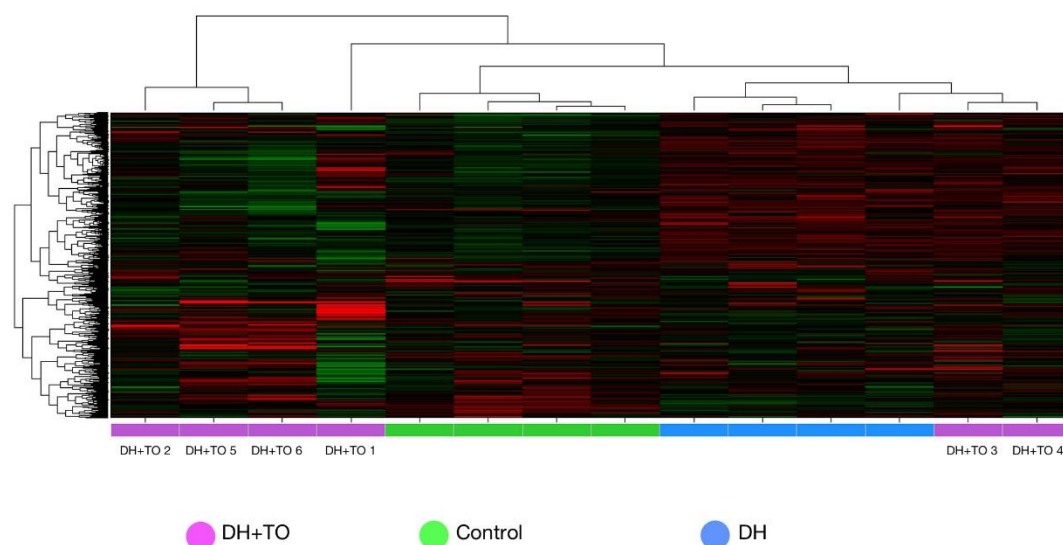
[Click here to Download Table S1](#)

Supplementary Table 2: Dataset of affected diseases and gene functions. The table gives an overview of the gene functions and categories that could be affected by the dysregulated genes of supplementary table 1.

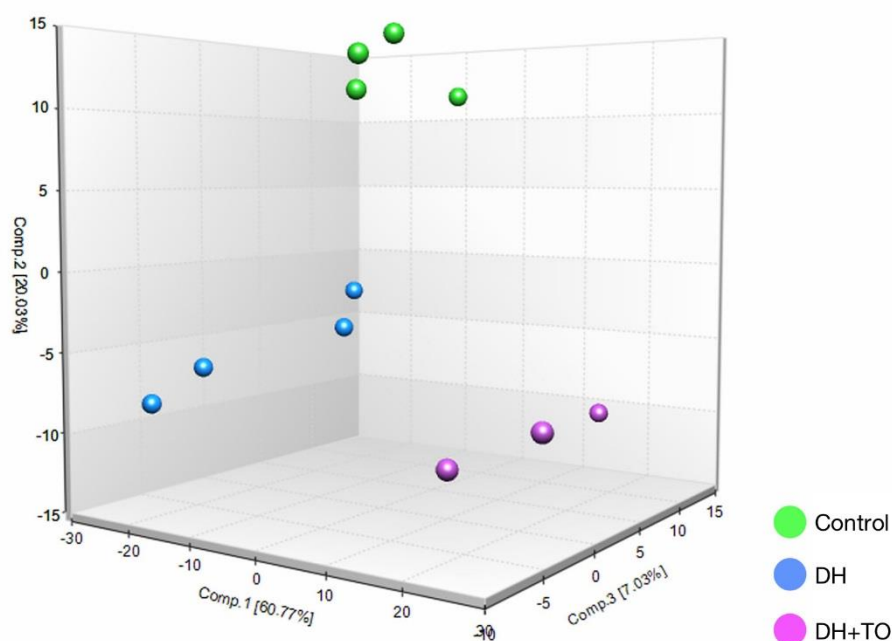
[Click here to Download Table S2](#)

Supplementary Table 3: List of genes investigated by qPCR, sequences of the forward and reverse primers and the corresponding PCR efficiencies.

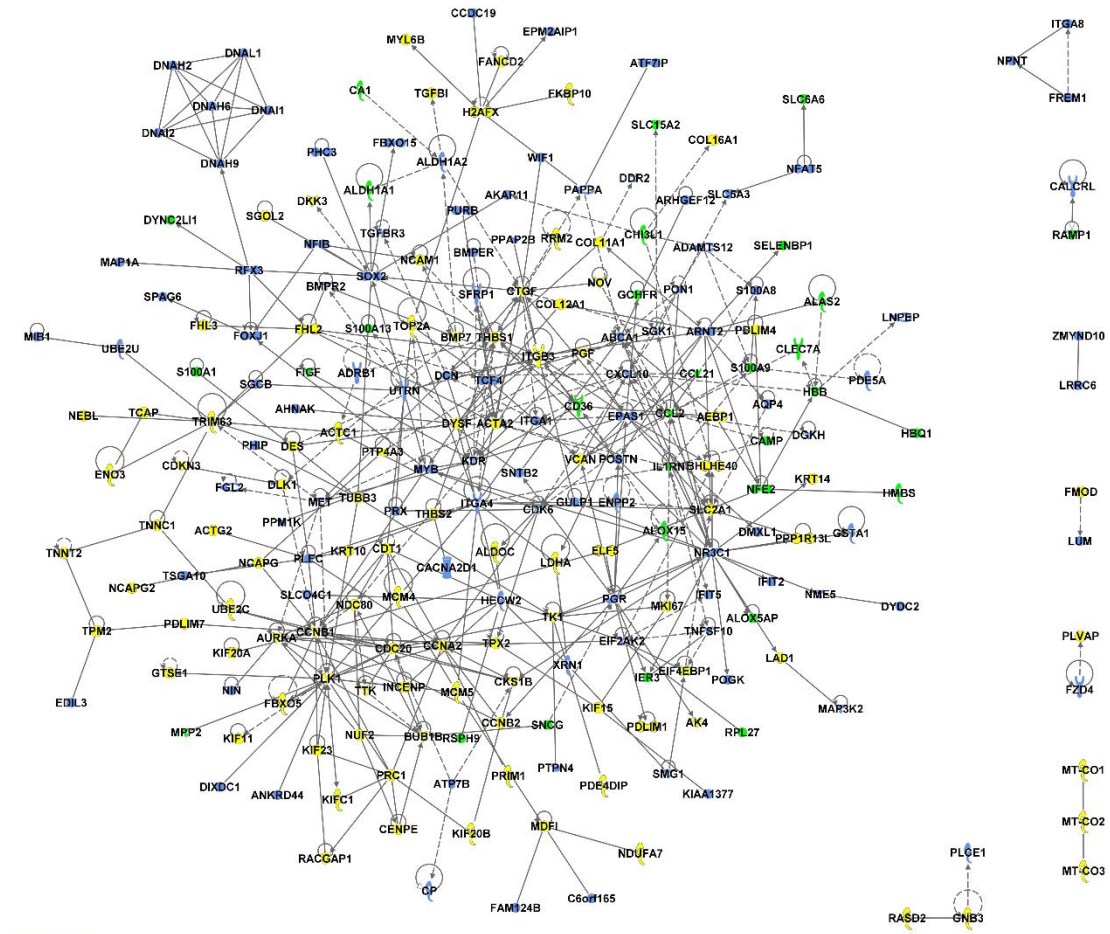
Gene name	Accession number	Forward Primer	Reverse primer	E	R ²
SDHA	ENSOCUG00000023573	CAGAACTGAAGACGGGAGGA	TCGCAGAGACCTTCCATACA	1.96	1
TOP1	ENSOCUG00000008221	TTCTCCAGTCCACCACGAAT	ATCCTCATCCCCGAGGTCTCT	2.04	0.999
GAPDH	ENSOCUG00000022054	GAGCTGAACGGGAAACTCAC	AGGTCAGGTCCACGACAGAC	1.95	0.998
RFX3	ENSOCUG00000014086	GCTCAGGTGCAGTATGTGGA	GGCTGTACATCTGGGTTTCTG	1.99	0.994
FOXJ1	ENSOCUG00000011472	GCCACCAAGATCACCTGT	GTTGTGGCGGATCGAGTT	2.01	0.999
PDE5A	ENSOCUG00000009417	CTTGGGCTACACCAACAACC	CCTCGGTTCAATGCAGAAGT	2.01	0.999
VEGFR2/KDR	ENSOCUG00000005062	GCAAGAAGGGTTTCAGCATC	GCTCACCAGCACGTCATAAA	2	0.999
ACTA2	ENSOCUG00000008193	CATCCAACCCTGTTGACTGA	GAGGCATAGAGGGACAGCAC	1.99	0.989
MKI67	ENSOCUG00000005133	AGGCAGGTGAACAAAAGACC	ATGAGCCCTCCCTATGACAA	1.97	0.996
WIF1	ENSOCUG00000014907	GTATGAACGGCGGACTTTGT	GTCCTGGTGGGCAAATACAT	2.02	0.997
BMPR2	ENSOCUG00000001971	TGTGAACCTGAGGGACTGTG	CAGATTCACCTGGGAAGAGG	1.96	0.999
LRRIQ1	ENSOCUG00000017527	AAGCCATTGTTCCAGTCC	CTGTCTGCACCTTTCTTCCA	2.08	0.999
SPAG17	ENSOCUG00000007586	CAGCTCCCAAGTTGCTAAA	CATCATCTGGCTCATCGTCA	2.04	0.999
CCDC39	ENSOCUG00000000812	ACCCGTTCTCTCTGAAACA	CCCTTTAGCCGTGACATTCT	2.06	0.981
VEGFR1/FLT1	ENSOCUG00000008523	GGCGATTACACCATCTTGCT	AGAGTCGGGTCTGGAAATGA	2.01	0.999



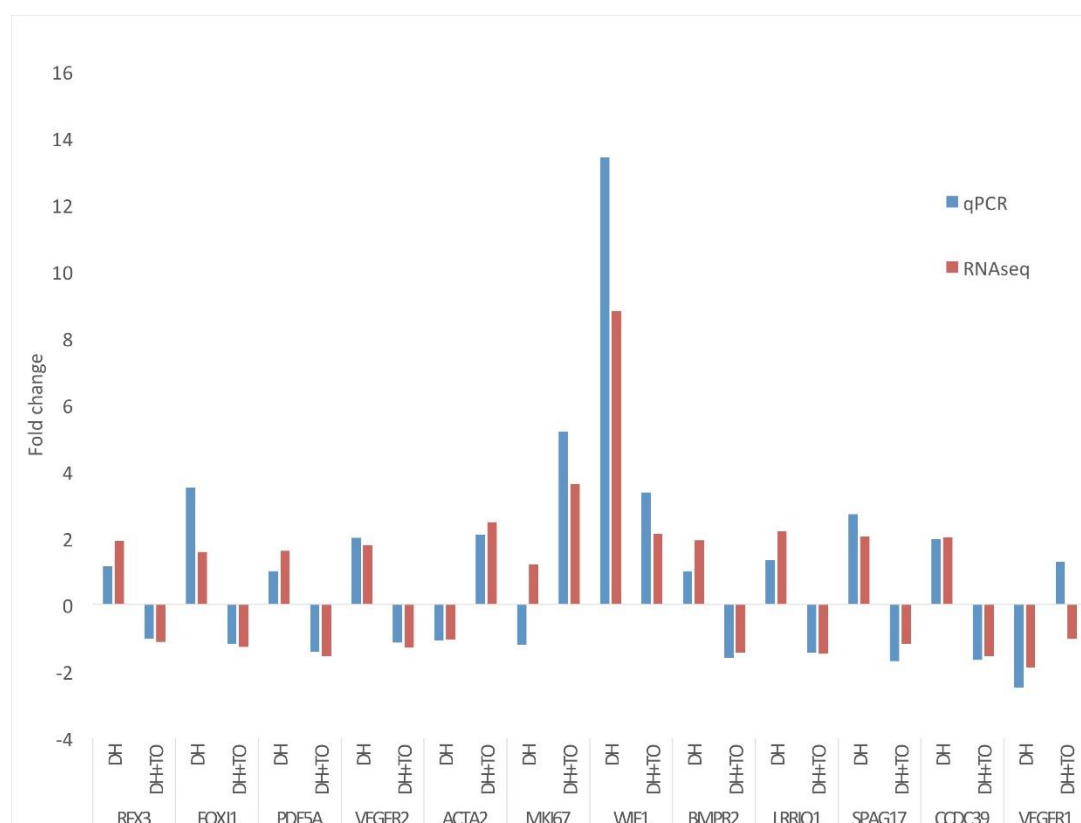
Supplementary Figure 1: Heatmap generated from unsupervised hierarchical clustering of all samples which underwent RNA-Seq. Samples are clustered horizontally, with TO in purple (n=6), Control in Green (n=4), and DH in Blue (n=4). Genes are clustered vertically, with red representing high expression and green representing low expression, with intensity corresponding to expression level. The Control and DH groups cluster together. Samples TO-3 and TO-4 cluster with the DH group and were removed from subsequent downstream analysis, as was sample TO-1 which was deemed a statistical outlier. The heatmap was generated using the Array Studio software, and was applied to Log₂ transformed RPKM expression values per gene for each sample which underwent RNA-Seq, and to all those 11,267 genes with expression values >1 RPKM (as described in the Methods section on the text).



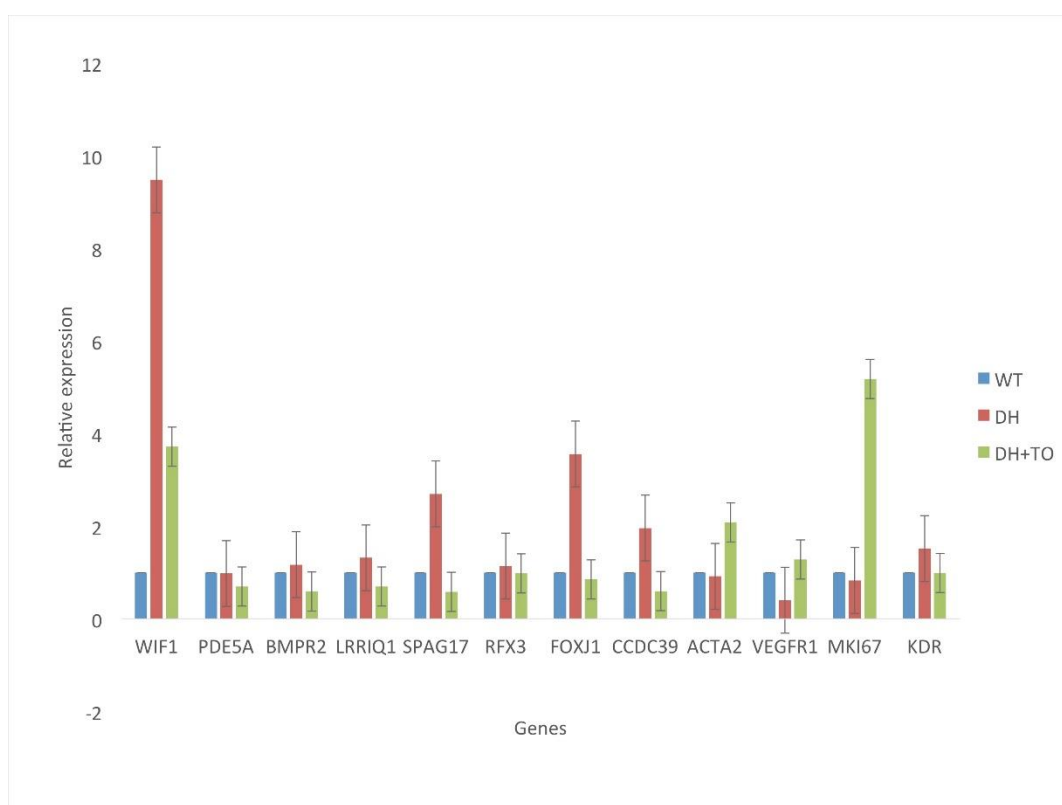
Supplementary Figure 2: Three dimensional PCA plot generated from those samples used for the downstream analysis. Samples are displayed according to component 1 (x-axis), component 2 (y-axis), component 3 (z-axis), with samples for TO in purple (n=3), Control in Green (n=4), and DH in Blue (n=4). The PCA plot was generated using the Array Studio software, and was applied to Log₂ transformed RPKM expression values per gene, for all those 641 genes which were dysregulated (as described in the Methods section of the text).



Supplementary Figure 3: Protein-Protein Interaction (PPI) network generated using the IPA web application. Molecules are linked where a known interaction exists, supported by evidence from the literature (i.e. not a predicted interaction). Molecules are coloured to represent the gene cluster in which they are found (see main text for further description of the gene clusters defined from the heatmap in Figure 1, and for which the data is given in Supplementary Table 1). Molecules in gene cluster 1 are coloured in yellow (low expression in both DH and control, and high expression in DH+TO only). Those molecules in gene cluster 2 are coloured in blue (high expression in DH only and low expression in control and DH+TO). Those molecules in gene cluster 3 are coloured in green (high expression in controls, and low expression in both DH and DH+TO). The PPI network was generated from the total of 641 unique genes found to be dysregulated (FC ± 2 ; FDR < 0.1) in any group comparison (see main text). 560 of 641 genes mapped within IPA to known functional genes. Molecules with evidenced interactions were linked and any orphan molecules (i.e. those not known to interact with any other in the dataset) were removed, generating the final PPI network displayed in which genes were color coded according to gene cluster.



Supplementary Figure 4: Fold changes of gene expression level in DH and DH+TO group, identified by qPCR and RNA seq. The figure shows similar gene expression variation between the two techniques. Values are shown in relation to the WT expressions.



Supplementary Figure 5: Relative expression determined by qPCR. The increase of LRRIQ1 and RFX3 in DH was not significant and there was no differential expression of BMPR2 and PDE5A in DH group.